Eur. Phys. J. Special Topics **225**, 2189–2206 (2016)

DOI: 10.1140/epjst/e2016-60058-2

THE EUROPEAN PHYSICAL JOURNAL SPECIAL TOPICS

Regular Article

Self-diffusiophoresis of chemically active colloids

Mihail N. Popescu[1,2,a], William E. Uspal[1,2,b], and Siegfried Dietrich[1,2,c]

[1] Max Planck Institute for Intelligent Systems, Heisenbergstr. 3, 70569 Stuttgart, Germany
[2] IV. Institut für Theoretische Physik, Universität Stuttgart, Pfaffenwaldring 57, 70569 Stuttgart, Germany

Received 20 February 2016 / Received in final form 19 April 2016
Published online 10 November 2016

Abstract. Chemically active colloids locally change the chemical composition of their solvent via catalytic reactions which occur on parts of their surface. They achieve motility by converting the released chemical free energy into mechanical work through various mechanisms, such as phoresis. Here we discuss the theoretical aspects of self-diffusiophoresis, which – despite being one of the simplest motility mechanisms – captures many of the general features characterizing self-phoresis, such as self-generated and maintained hydrodynamic flows "driven" by surface activity induced inhomogeneities in solution. By studying simple examples, which provide physical insight, we highlight the complex phenomenology which can emerge from self-diffusiophoresis.

1 Introduction

In the last decade there has been fast progress in the development of small objects (i.e., sizes in the micrometer range and smaller) endowed with means to be motile (self-propelled) in a liquid environment (see, e.g., Refs. [1–15]). Thorough and critical reviews of these rapid experimental developments are provided by Refs. [16–18]: the various motility mechanisms realized experimentally with chemically active colloids are discussed, with an emphasis on self-phoresis, by Refs. [16,17] and updated, with a stronger emphasis on the so-called micro-jets exhibiting "bubble propulsion" (motion by emission of bubbles), by the recent Ref. [18]. This is matched by a renewed interest on the theory side in the areas of motility at low Reynolds (Re) numbers (see, e.g., Refs. [19–25], which also review the earlier developments, as well as the minireview [26] in this topical issue) and of "active matter" in statistical physics. (Since these novel artificial "swimmers" operate under non-equilibrium conditions, they offer insights into off-equilibrium phenomena, such as, e.g., motility-induced phase transitions [27] or the formation of "living" crystals [9], which in general are very difficult to obtain.) The theoretical and numerical studies cover numerous issues ranging from the motility mechanisms at the single-particle level ("active particles") [28–49] to the

[a] e-mail: popescu@is.mpg.de
[b] e-mail: uspal@is.mpg.de
[c] e-mail: dietrich@is.mpg.de

emergence of complex collective behaviors ("active fluids"), such as swarming, phase separations, or chaotic turbulence [27,50–57].

One of the often encountered experimental realizations of self-propelled particles is that of colloidal particles with a surface chemistry designed such as to promote catalytically activated chemical reactions in the surrounding liquid environment [1–7,10,11]). Such particles, which we shall refer to as "chemically active colloids", achieve motility through various mechanisms of converting "chemical" free energy, obtained from locally changing the chemical composition of the environment via catalytic reactions,[1] into mechanical work. These include, e.g., bubble nucleation and pumping ("micro-jet engines", see Refs. [5,11]), or variants (diffusio-, electro-, electrochemical-) of phoresis [1–4,6,10,14] by exploiting the solvent mediated, effective interactions between the reactant and product molecules and the surface of the active particle [58]. Other fascinating examples of self-motility mechanisms are those of "hot Brownian" particles which move by inducing temperature gradients in the surrounding solution, discussed in the minireview [59] by Kroy et al. in this issue, and of the motion of drops due to Marangoni stresses, discussed in detail in the minireview [60] by Seemann et al. also in this issue.

In these notes we shall discuss the theoretical aspects of self-diffusiophoresis in solutions of electrically-neutral molecular species [58,61]. This is the simplest case of self-phoresis, yet it captures many of the general features of phoretic motility mechanisms. Aiming for a concise but insightful introduction to the topic, the presentation focuses on simplified models, which we expect to provide physical insight, and the complex phenomenology that can emerge from self-diffusiophoresis is illustrated via a few selected examples. Nevertheless, the theoretical framework is sufficiently detailed as to provide the interested reader with a good foundation to embark into further explorations of the field, starting from the references provided in these notes.[2]

2 Motility by self-diffusiophoresis

The classic review by Anderson has provided a unified description of various models of classical phoretic transport (such as electrophoresis, thermophoresis, and diffusiophoresis) in terms of "transport by interfacial forces". Accordingly, a steady-state motion of the particle relative to the solution emerges from the coupling between a non-equilibrium, externally maintained spatial variation of a thermodynamic field (e.g., electric potential, temperature, chemical potential or chemical composition) and the interaction of the molecules in solution with the colloid ("surface forces") [58].

While in the case of classic phoresis, non-equilibrium inhomogeneities are created and maintained externally, e.g., by placing the system in contact with two reservoirs at different chemical potentials, chemically active colloids create and maintain such inhomogeneities in chemical potential (and thus in the chemical composition of the solution) by catalytic chemical reactions they promote in the surrounding medium. These surface, catalytic chemical reactions are out of equilibrium, i.e., they operate unidirectionally; roughly speaking, the surface of the colloid turns into a "current injecting" (or "current withdrawing") boundary. One remark is in order here regarding

[1] Many of these experimental studies have employed the Pt-catalyzed decomposition of peroxide (H_2O_2) into water (H_2O) and oxygen (O_2) as the reaction of choice; we shall use it throughout the paper as an example for reactants and products, allowing us to obtain rough estimates for the values of various physical parameters, such as diffusion constants, required for the theoretical models.

[2] This list is by no means comprehensive, and we regret omitting many other contributions. In order to keep these notes concise, we have to pass to the interested reader the task of exploring the bibliography further via the reviews cited here.

the spatial variations in the composition of the solution. The non-equilibrium character of these variations in the composition of the solution, and therefore the existence of persistent currents of molecular species through the system, is essential. This point, elegantly highlighted in the study in Ref. [32], can be intuitively understood through the simple example of a chemically inert sphere immersed in a dilute solution (i.e., with a low number density c of the solute) interacting with the solute molecules via a potential $\Phi(\mathbf{r})$, which is not necessarily spherically symmetric. The system is taken to be thermostated. After a transient time, the system reaches an equilibrium state in which the solute density around the colloid attains the Boltzmann distribution: $c(\mathbf{r}) \sim \exp[-\beta\Phi(\mathbf{r})]$, with $\beta = 1/(k_B T)$, k_B the Boltzmann constant, and T the temperature. Thus the resulting equilibrium distribution $c(\mathbf{r})$ is spatially varying, and in general it is not spherically symmetric, yet the system is in thermodynamic equilibrium; therefore both the solution and the particle are motionless (except for thermal fluctuations).

It is important to estimate the "life-time" of these variations and compare it with the time scale set by the eventual motion of the particle. For molecular species such as O_2, at room temperature the diffusion constant D in liquids such as water is of the order of 10^{-9} m^2/s. Thus the diffusion time t_{diff} over a length comparable with the radius $R \sim 10^{-6}$ m of the colloid is $t_{diff} = R^2/D \sim 10^{-3}$ s. The experiments with chemically active colloids report typical velocities of the colloid $U \lesssim 10$ μm/s, and thus one infers characteristic "drift" times $t_{drift} = R/U \gtrsim 10^{-1}$ s $\gg t_{diff}$. (Due to its large size, the translational and rotational diffusion times of the colloid are order of magnitude larger than t_{diff}.) Therefore one can indeed expect that the chemical activity may induce, via fast molecular diffusion, a quasi-steady state around the colloid and thus a situation which resembles an "externally-maintained" variation in the chemical composition.

The considerations above lead to the conclusion that the conditions for a "self-induced" phoresis may be met by the chemically active colloids. We thus proceed by identifying the key components, which are present in any experimental realization of self-phoretic colloids. This allows us to formulate a *minimal theoretical model* of chemically active colloids, exhibiting self-diffusiophoresis as the conceptually simplest type of self-phoretic motion.[3]

(i) Chemical activity: The simplest model of a reaction involving the particle and the solution is the one in which a solvent molecule contacting the particle surface is converted with a certain probability to a solute molecule; this defines an effective reaction rate. This condition, together with particle reservoirs for solvent and solute species and diffusion of solute molecules, provides for steady state non-equilibrium variations in the chemical composition.

(ii) Colloid-solution interactions: The solute molecules interact with the colloid via a potential which differs from the potential characterizing the interaction of the solvent molecules with the colloid. Thus the notations of "solute" and "solvent" have a meaning beyond that of mere labels applied to otherwise identical molecular species.

[3] It does not require much argument to realize that modeling a system with non-uniform temperature (thermophoresis) is clearly a more challenging task; likewise dealing with an electrolyte (charged species, electrophoresis) rather than with an electrically neutral system.

(iii) Asymmetry: For motion of the colloid to occur, the system consisting of the particle plus the solution with inhomogeneous chemical composition must possess some degree of spatial asymmetry. (Here we do not consider the occurrence of spontaneous symmetry breaking.) The most common sources of spatial asymmetry are: a spatially-inhomogeneous activity (i.e., only parts of the colloid surface posses catalytic properties), a reduced symmetry of the shape of the colloid, or motion near boundaries (walls or interfaces) which intrinsically distort the spatial variations of the chemical composition.

Following these lines one eventually arrives at the basic model of self-diffusiophoresis proposed by Golestanian et al. [28] and analyzed further in Refs. [30, 32,34–38,40]. In spite of its relative simplicity, this model has been shown to capture the phenomenology encountered experimentally for polystyrene spheres partially covered by Pt and immersed in H_2O_2 aqueous solutions[4] [7,37]. We shall discuss this model in further detail in the present section and use it in, c.f., Sects. 3 and 4 in order to highlight some of the complex behaviors exhibited if self-diffusiophoretic motion couples with boundaries or external fields.

2.1 Minimal model of self-diffusiophoresis

We consider a chemically active colloidal particle of linear size $R \sim 1\ \mu$m (where R can be defined as $\max|\mathbf{r}_1 - \mathbf{r}_2|/2$, $\mathbf{r}_{1,2} \in \mathcal{S}_p$, with $\mathcal{S}_p$ denoting the surface of the particle, or, equivalently, via the radius of the smallest sphere that includes the colloid within its volume) which is suspended in an unbounded, incompressible Newtonian liquid solution of, to a very good approximation, constant mass density ρ and viscosity μ (see Fig. 1(a)). The particle is assumed to be neutrally buoyant; the case in which gravity plays a role will be briefly discussed in, cf., Sect. 4. At the time $t = 0$ (i.e., before the chemical activity of the colloid is "turned on"), the solution is quiescent and consists of solvent molecules only. A part $\mathcal{S}_c$ of the surface or the whole surface of the particle is "chemically active", e.g., by being covered with a catalyst; once the chemical activity is "turned on", the part $\mathcal{S}_c$ of the particle promotes the irreversible conversion of solvent molecules S into molecules of species A, $S \to A$, with a "reaction" rate k which is constant in time and space.[5] Furthermore, both the solute molecules of species A and the solvent molecules are assumed to be much smaller than the colloid, such that they can be approximated as point particles and the solution can be treated as a continuum. The A molecules diffuse in solution with diffusion coefficient D, and the number density of the A species is taken to be very small compared to the number density of the solvent (corresponding to a dilute ideal solution) such that in solution the interaction between the A molecules is negligible. The interactions of the A molecules with the solvent molecules and those between the solvent molecules are encoded in the viscosity μ of the solution. We take the solution to be in contact with a reservoir of solvent molecules S and with a reservoir of product molecules A which, far from the particle, maintain a constant number density c_S for the solvent

[4] However, there is a significant debate on whether or not the reaction mechanism in these particular experimental realizations can indeed be mapped onto a simple production of an electrically neutral molecular solute [62,63].

[5] For simplicity, we consider the case in which the solvent is also the reactant and there is a single product molecular species emerging from the chemical reaction [38]. The case in which several species are involved in the chemical reaction can be analyzed along similar lines (see, e.g., Refs. [40,49]). But it requires a more cumbersome algebra and possesses potential conceptual complications which arise from dealing with multi-component mixtures and from the interplay of several different molecular masses and interaction potentials [64].

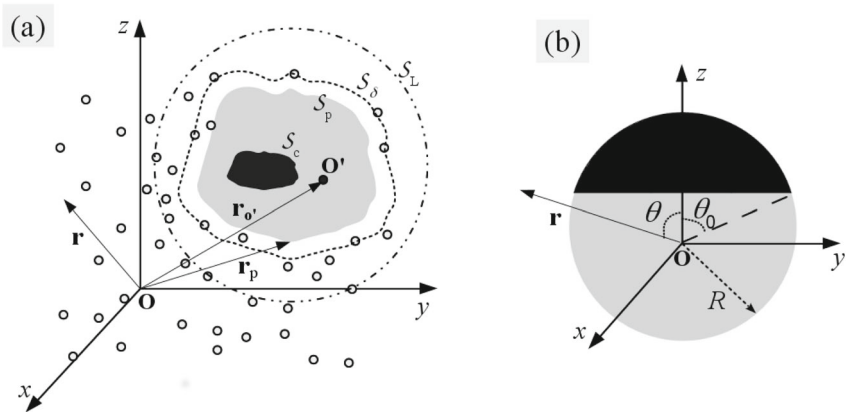

Fig. 1. (a) Schematic (and not to scale) illustration of a colloidal particle, which has a chemically inhomogeneous surface $\mathcal{S}_P$, immersed in an unbounded solution. The "active" part $\mathcal{S}_c$ (black area) of the surface $\mathcal{S}_P$ of the particle catalyzes upon contact a chemical transformation of solvent molecules S (not depicted) into product (solute) molecules A (small grey circles) which diffuse in the solution. The part $\mathcal{S}_P \setminus \mathcal{S}_c$ (grey area) is chemically inactive. O' denotes the center of mass of the particle. (For the definitions of $\mathcal{S}_\delta$ and $\mathcal{S}_\mathrm{L}$ see the main text.) (b) Schematic illustration of a spherical "Janus colloid". As in (a), black (grey) indicates the chemically active (inactive) regions. The catalytic area is a spherical cap (of a size determined by the radius R and the opening angle θ_0); thus the physical properties of the surface exhibit axial symmetry with respect to the axis (Oz) passing through the centers of the particle and the cap.

molecules and a constant number density c_0 for the solute molecules. We assume that the diffusion constant D_s of the solvent molecules is sufficiently large such that the reaction is the rate limiting step of the conversion (i.e., the Damköhler number $Da \simeq kR/D_s$ is assumed to be very small, see, e.g., Ref. [65]). Under these conditions, the reaction on the colloid surface $\mathcal{S}_c$ effectively acts solely as a source releasing solute molecules A into the solution. (Note that by the definition of this model, the solute remains at all times dissolved in the solution; i.e., we do not consider here the cases in which it can phase separate as in, e.g., the bubble-propulsion of micro-objects as reported in Refs. [5,11].)

Finally, it is assumed that the interaction of a (point-like) molecule of species S (A), located at $\mathbf{r}$, with the colloid is described by the potential $\phi_{S(A)}(\mathbf{r})$, and we denote by $\Phi(\mathbf{r}) = \phi_A(\mathbf{r}) - (m_A/m_S)\phi_S(\mathbf{r}) = \phi_A(\mathbf{r}) - \phi_S(\mathbf{r})$ the interaction potential of A molecules with the colloid relative to that of the solvent molecules. (Here m_S and m_A are the molecular masses of the solute and solvent molecules, respectively; for the system described above, mass conservation in the reaction requires $m_S = m_A$.) The typical molecule-colloid interaction potentials Φ (e.g., the van der Waals interaction) are steeply decreasing functions of the distance from the surface of the colloid ($\Phi(|\mathbf{r}| \to \infty) \to 0$), and therefore one can generally find a surface $\mathcal{S}_\delta$ enclosing the colloid such that $\beta\Phi(\mathbf{r}) \ll 1$ and $|\nabla\Phi(\mathbf{r})| \approx 0$ for $\mathbf{r}$ outside the domain enclosed by $\mathcal{S}_\delta$. The domain (of volume $\mathcal{V}_\delta$) delimited by $\mathcal{S}_P$ and $\mathcal{S}_\delta$, where the solute-colloid interactions are relevant, will be called "surface film". (Note that, following the terminology in Ref. [58], this domain is often called "interfacial layer".) In order that the surface of the particle is impenetrable to the solvent and solute molecules, it is necessary that $\phi_{S(A)}(\mathbf{r}) \to +\infty$ for $\mathbf{r} \in \mathcal{V}_p$, where $\mathcal{V}_p$ denotes the volume enclosed by $\mathcal{S}_P$. Furthermore, we will assume that the potential $\Phi(\mathbf{r})$ is such that for $\mathbf{r}$ outside $\mathcal{V}_P$ it satisfies $\Phi(\mathbf{r} \to \mathbf{r}_P) = +\infty$, i.e., near the surface of the particle the solvent molecules are preferred over the solute molecules.

2.2 Motion of particles, diffusion of solutes, and hydrodynamics of the solution

Due to the interaction encoded in $\Phi(\mathbf{r})$, a fluid element $\delta\mathcal{V}$ located at $\mathbf{r}$ experiences a force $\mathbf{f}\delta\mathcal{V}$, where the force density is given by $\mathbf{f} = -c(\mathbf{r})\nabla\Phi(\mathbf{r})$. (This follows from the total force density $\mathbf{f}_{tot} = -(c_s\nabla\phi_S + c\nabla\phi_A)$ by: using that the mass density ρ of the solution is constant, which allows one to express c_s in terms of ρ and c; then separating $\mathbf{f}_{tot}$ into $\mathbf{f}$ and a gradient term involving only ϕ_S. The latter term is then included in the definition of the pressure p of the solution and thus no longer appears explicitly in the calculations, see, e.g., Ref. [40].) According to Newton's third law, the solute molecules in the fluid element $\delta\mathcal{V}$ exert a force of equal magnitude but of opposite sign $-\mathbf{f}\delta\mathcal{V}$ on the colloid. ($|\int_{\mathcal{V}_\infty}\mathbf{f}\delta\mathcal{V}|$, where $\mathcal{V}_\infty$ denotes the volume of the solution, thus quantifies the magnitude of the force exerted by the solute distribution on the colloid. For typical interaction potentials $\Phi(\mathbf{r})$ the integral is bounded [38,40], i.e., the colloid experiences – as expected – a finite force.) Therefore, both the solution and the colloid are subject to distributed forces. If free to move, they may achieve a state of relative motion in which the colloid moves as a rigid body with translational and rotational velocities $\mathbf{V}$ and $\mathbf{\Omega}$, respectively, while a hydrodynamic flow $\mathbf{u}(\mathbf{r})$ is induced in the solution. Since the distribution of forces is determined by the distribution $c(\mathbf{r})$ of the number density of solute molecules, we start by studying the latter.

Due to the fact that in the solution (i.e., outside the surface of the colloid and inside the container located at a macroscopic distance from the colloid) there are no reactions involving the solute, there are no sources or sinks of solute in the bulk. Since, as discussed above, the diffusion of the solute is very fast, a quasi-steady-state distribution (around the current position of the particle) is established over time scales much shorter than that of the macroscopic motion of the colloid. Accordingly, $c(\mathbf{r})$ satisfies the steady-state conservation law

$$\nabla\cdot\mathbf{J} = 0\,, \tag{1}$$

where the current of solute molecules

$$\mathbf{J} = c(\mathbf{r})\,\mathbf{u}(\mathbf{r}) - D\,\nabla c(\mathbf{r}) - D\,c(\mathbf{r})\nabla(\beta\Phi(\mathbf{r})) \tag{2}$$

accounts for the advection of the solute by the flow of the solution, the diffusion due to the density gradients, and the drift of the solute molecules due to their interaction with the colloid [38,40,64,65]. The relative magnitude of the advection and the diffusion currents is characterized by the Péclet number $Pe = |\mathbf{V}|R/D$, where $\mathbf{V}$ is the velocity of the colloid. For typical values $|\mathbf{V}| \sim 1 - 10\,\mu$m/s as observed experimentally and for $D \sim 10^{-9}\,\mathrm{m}^2/\mathrm{s}$ as discussed above, for a particle of $R = 1\,\mu$m the typical Péclet numbers are in the range $Pe \sim 10^{-3} - 10^{-1}$. Therefore, in typical cases the advection of the solute is negligible. This implies a major simplification of the problem because it effectively leads to a decoupling of the dynamics of the solute distribution from that of the flow of the solution.[6] By combining Eqs. (1) and (2), neglecting the advection component, and adding the appropriate boundary conditions we arrive at the following boundary-value problem for the field $c(\mathbf{r})$:

$$\nabla\cdot[\nabla c(\mathbf{r}) + c(\mathbf{r})\nabla(\beta\Phi(\mathbf{r}))] = 0\,, \tag{3a}$$

$$c(|\mathbf{r}|\to\infty)\to c_0\,, \tag{3b}$$

and

$$-D\{\mathbf{n}\cdot[\nabla c(\mathbf{r}) + c(\mathbf{r})\nabla(\beta\Phi(\mathbf{r}))]\}|_{\mathcal{S}_P} = K(\mathbf{r}_P)\,. \tag{3c}$$

[6] For a more rigorous discussion of this point see Ref. [38], while for a thorough discussion of the corrections at non-vanishing Pe numbers see Ref. [65].

Here and in the following $\mathbf{n}$ denotes the normal to the corresponding surface oriented *into* the fluid. The boundary condition in Eq. (3c) encodes the activity of the particle by equating the solute current along the normal to the surface with a source function $K(\mathbf{r}_P) > 0$ which accounts for the conversion of solvent molecules into solute molecules at those parts of the surface that are catalytic ($\mathbf{r}_P \in \mathcal{S}_c$). At the points $\mathbf{r}_P$ belonging to the inert part one has $K(\mathbf{r}_P) = 0$. (An "annihilation" of the solute molecules over certain parts of the surface could be included by allowing for $K(\mathbf{r}_P) < 0$ over that part [30,38].)

The hydrodynamic flow of the solution is described by the Navier-Stokes equations subject to appropriate boundary conditions. A significant simplification of this problem is possible by estimating, guided by the values observed in experimental studies of chemically active particles, the corresponding Reynolds number defined as $Re = \rho R|\mathbf{V}|/\mu$. By using for ρ and μ the values corresponding to water at room temperature, $R \sim 1\,\mu$m, and $|\mathbf{V}| \lesssim 10\,\mu$m/s one arrives at $Re \lesssim 10^{-5}$. Thus the hydrodynamic flow $\mathbf{u}(\mathbf{r})$ can be obtained from the solution of the incompressible Stokes equations with a body force density $\mathbf{f} = -c(\mathbf{r})\nabla\Phi(\mathbf{r})$ subject to boundary conditions of a quiescent solution far from the colloid and no-slip on the surface of the colloid, i.e.,

$$\nabla \cdot \overleftrightarrow{\sigma} - c(\mathbf{r})\nabla\Phi(\mathbf{r}) = 0\,, \qquad \nabla \cdot \mathbf{u}(\mathbf{r}) = 0\,, \tag{4a}$$

$$\mathbf{u}(|\mathbf{r}| \to \infty) = 0\,, \tag{4b}$$

$$\mathbf{u}(\mathbf{r}_P) = \mathbf{V} + \boldsymbol{\Omega} \times (\mathbf{r}_P - \mathbf{r}_{O'})\,, \ \mathbf{r}_P \in \mathcal{S}_P\,, \tag{4c}$$

where

$$\overleftrightarrow{\sigma} := -p\mathsf{I} + \mu\left[\nabla\mathbf{u} + (\nabla\mathbf{u})^\dagger\right] \tag{5}$$

is the stress tensor in the solution, $p(\mathbf{r})$ is the pressure, and I is the identity tensor.

Equations (3) and (4), which are coupled (weakly) by the force density term in Eq. (4a), must be supplemented by additional conditions in order to determine the as yet unknown velocities $\mathbf{V}$ and $\boldsymbol{\Omega}$, which enter via the boundary conditions in Eq. (4). This is provided by a closure condition imposed by the balance of forces and torques acting on the colloid. In the absence of external forces ($\mathbf{F}_{ext} = 0$) and external torques ($\mathbf{T}_{ext} = 0$)[7], this takes the form

$$\int_{\mathcal{S}_P} dS\, \overleftrightarrow{\sigma} \cdot \mathbf{n} + \int_{\mathcal{V}_\infty} d\mathcal{V}\, c(\mathbf{r})\nabla\Phi(\mathbf{r}) = -\mathbf{F}_{ext} = 0\,, \tag{6a}$$

$$\int_{\mathcal{S}_P} dS\, (\mathbf{r}_P - \mathbf{r}_{O'}) \times (\overleftrightarrow{\sigma} \cdot \mathbf{n}) + \int_{\mathcal{V}_\infty} d\mathcal{V}\, (\mathbf{r} - \mathbf{r}_{O'}) \times [c(\mathbf{r})\nabla\Phi(\mathbf{r})] = -\mathbf{T}_{ext} = 0. \tag{6b}$$

Thus, the hydrodynamic boundary conditions at the surface of the particle, determined by $\mathbf{V}$ and $\boldsymbol{\Omega}$, must be chosen such that the resultant flow obeys the relations in Eq. (6). Finally, one notes that under the approximation of vanishing forces outside the domain delimited by $\mathcal{S}_\delta$ (see Fig. 1(a)) the volume integrals over $\mathcal{V}_\infty$ are approximately equal to volume integrals over $\mathcal{V}_\delta$. By applying the divergence theorem to

[7] If there are external forces or torques acting on the particle, the linearity of the Stokes equations allows one to account for their effects separately via standard procedures. The examples presented in Sect. 4.1 illustrate this point.

Eq. (4a) integrated over the volume delimited by $\mathcal{S}_P$ and any surface, in particular $\mathcal{S}_L$ of a sphere, enclosing $\mathcal{S}_\delta$ (see Fig. 1(a)), one can reformulate Eq. (6) as

$$\int_{\mathcal{S}_L} dS \overleftrightarrow{\sigma} \cdot \mathbf{n} \simeq 0\,, \qquad \int_{\mathcal{S}_L} dS\,(\mathbf{r} - \mathbf{r}_{O'}) \times (\overleftrightarrow{\sigma} \cdot \mathbf{n}) \simeq 0\,. \tag{7}$$

This is a condition of zero hydrodynamic force and torque exerted by the flow $\mathbf{u}(\mathbf{r})$ on any surface $\mathcal{S}_L$ enclosing the surface film. (Actually this is an approximate relation which relies on effectively neglecting $|\nabla\Phi(\mathbf{r})|$ outside the surface film. True equalities hold upon the replacement $\mathcal{S}_L \to \mathcal{S}_\infty$ [40,58,65].)

By solving the coupled Eqs. (3), (4), and (6) (or (7)), in principle one can obtain the linear and angular velocities of the particle, as well as the distribution of solute and the hydrodynamic flow field of the solution. However, in practice this is a very difficult problem, particularly because the Stokes equations have to be solved with *a priori* unknown boundary conditions (since $\mathbf{V}$ and $\mathbf{\Omega}$ are initially unknown) which then must be adjusted until the condition in Eq. (6) is satisfied. Even for the simpler case of a spherical Janus colloid (see Fig. 1(b)) this turns out to be a very difficult problem, which can be solved only approximately in terms of a perturbation series [40]. If one is interested only in the velocities $\mathbf{V}$ and $\mathbf{\Omega}$, the complication described above can be bypassed (at the expense of leaving the hydrodynamic flow $\mathbf{u}(\mathbf{r})$ unknown) by applying the generalized Lorentz theorem [66], as carried out for a spherical surface in Ref. [38]. The interested reader is encouraged to follow up on this point, guided by Ref. [38]. We shall discuss the Lorentz theorem below in the context of particles for which the surface film is very thin. Specific examples of using this formulation will be provided in, cf., Sects. 3 and 4.

2.3 The thin surface film approximation and phoretic slip

Further progress can be made if the potential $\Phi(\mathbf{r})$ has a very short range, i.e., if the thickness δ of the surface film is very small compared with the macroscopic length scales set by the size of the particle R and by the minimal radius of curvature of $\mathcal{S}_P$. Furthermore, one assumes that $\Phi(\mathbf{r})$ varies only weakly along the surface, while the variations in the direction normal to the surface are large because it decays to zero within the distance δ. Under these conditions, treating both the diffusion and hydrodynamics via asymptotic matching on $\mathcal{S}_\delta$ of an *inner* (within the surface film) and *outer* solution reduces the initial problem to that of solving in the outer domain the Laplace (diffusion) equation and the force free, incompressible Stokes (hydrodynamics) equation, respectively. A detailed presentation of this approach can be found in Anderson's classic review of phoresis [58]. Thus here we shall only concisely discuss the main points.

Under the thin surface film assumptions formulated above, at any point $\mathbf{r}_P \in \mathcal{S}_P$ we can define a rectangular region of thickness δ and mesoscopic "in plane" size (i.e., its lateral extension is much smaller than R but much larger that δ). In this planar geometry, for which one introduces cylindrical coordinates (ζ, Φ, h) with the origin at $\mathbf{r}_P$ (h denoting the vertical coordinate, ζ the radial one, and Φ the polar angle), the inner problem for diffusion renders a rapid relaxation of the solute density along the direction normal to the surface towards the equilibrium Boltzmann distribution. The latter is determined by the local potential $\Psi(h; \mathbf{r}_P) = \Phi(\mathbf{r})$, where $\mathbf{r} = \mathbf{r}_P + h\,\mathbf{e}_h$, which is defined under the above assumption that Φ does not vary laterally over these mesoscopic scales. This implies $c_{in}(\zeta, h) = c_{out}(\zeta) \exp[-\beta\Psi(h; \mathbf{r}_P)]$, where $c_{out}(\zeta)$ is the solution of the outer problem evaluated at $\mathcal{S}_\delta$, matching $c_{in}(\zeta, h \to \infty)$.

The hydrodynamic problem in the inner domain is solved in the lubrication approximation, accounting for the fact that, via the prefactor $c_{out}(\zeta)$, the variation of the solute distribution in the direction ζ translates into a variation of the osmotic pressure along the surface and thus drives hydrodynamic flow parallel to the surface [58]. The final result of the analysis of the dynamics in the thin surface film is that at the outer surface $\mathcal{S}_\delta$ one obtains a boundary condition for the hydrodynamics in the outer domain (for which $\mathcal{S}_\delta$ is the inner boundary) in the form of a prescribed *phoretic* slip. This is determined by the number density distribution of solute obtained from the analysis in the outer domain and by the potential Ψ:

$$\mathbf{u}_s(\mathbf{r}_P) = -\frac{\mathcal{L}(\mathbf{r}_P)}{\beta\mu}\nabla_{||}c(\mathbf{r}_P) := -b(\mathbf{r_P})\nabla_{||}c(\mathbf{r}_P)\,, \tag{8a}$$

where

$$\mathcal{L}(\mathbf{r}_P) = \int_0^\infty dh\, h\,\{\exp\left[-\beta\Psi(h;\mathbf{r}_P)\right] - 1\} \tag{8b}$$

and $\nabla_{||}$ denotes the projection of ∇ onto the tangent plane of the surface. As indicated above, $\mathcal{L}$ (which has the units of an area) and thus the "phoretic mobility" $b(\mathbf{r_P})$, which has the units of m^5/s, may depend on the position along the surface. This accounts for, e.g., the catalyst covered part of the surface interacting with the solute molecules differently than the inert part. The quantity $\mathcal{L}$ entering into the definition of the phoretic slip deserves further discussion. As discussed above, the potential $\Psi(h;\mathbf{r}_P)$ is repulsive (positive) at $h \to 0$ and decays to zero at large distances. Therefore, in general the potential can be either repulsive at all distances, or it can become attractive beyond a certain distance h_0. In this latter case it exhibits an attractive minimum which corresponds to *adsorption* of the solute. Thus one has $\mathcal{L} < 0$ (i.e., $b < 0$) for purely repulsive interactions $\Psi(h)$. If, however, $\Psi(h)$ has an attractive part, h_0 is sufficiently small, and the attractive minimum is sufficiently deep, one can have $\mathcal{L} > 0$ (i.e., $b > 0$). For the rest of the notes, the notion "attractive interactions" will refer strictly to the latter case, i.e., potentials $\Psi(h)$ which have attractive parts and satisfy $\mathcal{L} > 0$.

In the limit of thin surface films, the Eqs. (3), (4), and (7), which govern self-diffusiophoresis, take the form

$$\nabla^2 c(\mathbf{r}) = 0\,, \tag{9a}$$

$$-D\,[\mathbf{n}\cdot\nabla c(\mathbf{r})]|_{\mathcal{S}_\delta \simeq \mathcal{S}_P} = K(\mathbf{r}_P)\,, \tag{9b}$$

$$c(|\mathbf{r}| \to \infty) \to c_0\,, \tag{9c}$$

and

$$\nabla\cdot\overset{\leftrightarrow}{\sigma} = 0\,, \qquad \nabla\cdot\mathbf{u}(\mathbf{r}) = 0\,, \tag{10a}$$

$$\mathbf{u}(\mathbf{r})|_{\mathcal{S}_\delta\simeq\mathcal{S}_P} = \mathbf{u}_s(\mathbf{r}_P) + \mathbf{V} + \mathbf{\Omega}\times(\mathbf{r}_P - \mathbf{r}_{O'})\,,\ \mathbf{r}_P \in \mathcal{S}_P\,, \tag{10b}$$

$$\mathbf{u}(|\mathbf{r}| \to \infty) = 0\,, \tag{10c}$$

with $\mathbf{u}_s$ given by Eqs. (8a) and (8b), while the boundary conditions are imposed at (approximately) the surface $\mathcal{S}_P$ (because at the length scales of the outer problem

$\mathcal{S}_\delta$ is infinitesimally close to $\mathcal{S}_P$), and with the zero-force and zero-torque conditions implemented also formally at $\mathcal{S}_P$ (but actually at $\mathcal{S}_\delta$):

$$\int_{\mathcal{S}_P} dS \overset{\leftrightarrow}{\sigma} \cdot \mathbf{n} \simeq 0\,, \qquad \int_{\mathcal{S}_P} dS\,(\mathbf{r}_P - \mathbf{r}_{O'}) \times (\overset{\leftrightarrow}{\sigma} \cdot \mathbf{n}) \simeq 0\,. \tag{11}$$

Although the resulting equations are simpler, the complications, due to *a priori* unknown boundary conditions in the hydrodynamics problem, persist.

As stated above, the velocities $\mathbf{V}$ and $\boldsymbol{\Omega}$ can actually be determined without solving the full problem by employing the Lorentz reciprocal theorem [66–68]. This states that any two flow fields $\mathbf{u}(\mathbf{r})$ and $\mathbf{u}_a(\mathbf{r})$, which are solutions of the force-free, incompressible Stokes equations within the same domain $\mathcal{D}$, obey the relation

$$\int_{\partial\mathcal{D}} \mathbf{u} \cdot \overset{\leftrightarrow}{\sigma}_a \cdot \mathbf{n}\, dS = \int_{\partial\mathcal{D}} \mathbf{u}_a \cdot \overset{\leftrightarrow}{\sigma} \cdot \mathbf{n}\, dS\,, \tag{12}$$

where $\overset{\leftrightarrow}{\sigma}$ and $\overset{\leftrightarrow}{\sigma}_a$ denote the stress tensors corresponding to the two flow fields and $\partial\mathcal{D}$ the surface enclosing the domain $\mathcal{D}$.

We apply the Lorentz theorem to our system by choosing $\mathbf{u}$ to be the flow solving Eq. (10) and $\mathbf{u}_a$ (the so called "auxiliary problem") to be the flow corresponding to a chemically inert particle (i.e., no phoretic slip: $\mathbf{u}_s^{(a)} = 0$) moving with prescribed velocities $\mathbf{V}_a$ and $\boldsymbol{\Omega}_a$. Such an auxiliary problem can be straightforwardly solved either analytically (for simple shapes like spheres or spheroids) or numerically (e.g., by using the Boundary Element Method (BEM) [45,69]). The domain in our case is delimited by $\mathcal{S}_\delta \simeq \mathcal{S}_P$ and the surface $\mathcal{S}_\infty$ at infinity. Noting that with increasing distance from the particle both $\mathbf{u}$ and $\mathbf{u}_a$ must decay at least as $1/|\mathbf{r}|$, the integrals over $\mathcal{S}_\infty$ vanish and thus in Eq. (12) only the integrals over $\mathcal{S}_P$, where the flows are prescribed by the boundary conditions, remain. Exploiting the fact that $\mathbf{V}$, $\boldsymbol{\Omega}$, $\mathbf{V}_a$, and $\boldsymbol{\Omega}_a$ are constant vectors, and using Eq. (11), one arrives at

$$\mathbf{V} \cdot \mathbf{F}_a + \boldsymbol{\Omega} \cdot \mathbf{T}_a = -\int_{\mathcal{S}_P} \mathbf{u}_s \cdot \overset{\leftrightarrow}{\sigma}_a \cdot \mathbf{n}\, dS\,, \tag{13}$$

where $\mathbf{F}_a$ and $\mathbf{T}_a$ are the hydrodynamic force and torque on the particle exerted by the auxiliary flow $\mathbf{u}_a$. In Eq. (13) the unknowns $\mathbf{V}$ and $\boldsymbol{\Omega}$ are now isolated, rather than being implicit as in the initial formulation, while all the other terms are known, following from the solution of the auxiliary problem. Therefore, by selecting six linearly independent auxiliary problems (of the form discussed above) and formulating for each of them Eq. (13) with the corresponding $\mathbf{F}_a$, $\mathbf{T}_a$ and with the integral on the rhs, one obtains a system of six linear equations for the six components of $\mathbf{V}$ and $\boldsymbol{\Omega}$ as the unknowns. This concludes the solution.

The calculation above is greatly simplified for particles with shapes and catalyst decoration exhibiting a high degree of symmetry. Examples are Janus spheres (see Fig. 1(b)), cylinders, spheroids, or dumbbells. In these cases various components of $\mathbf{V}$ and $\boldsymbol{\Omega}$ can be shown to vanish due to the symmetry of the problem, and for these shapes analytic solutions for translations or rotations in quiescent fluids are known. Such calculations are discussed in, e.g., Refs. [28,30,34,44,65]. We concisely present as an example the Janus sphere shown in Fig. 1(b), which is one of the chemically active colloids frequently used in experimental studies [7,10,16]. Due to the axial symmetry of the system, one can infer that $\boldsymbol{\Omega} = 0$ and the only possible motion is a translation with velocity $\mathbf{V} = V\mathbf{e}_z$ along the z-axis (see Fig. 1(b)). Choosing the

auxiliary problem to be that of a chemically inert sphere translating with velocity $\mathbf{V}_a = V_a \mathbf{e}_z$, which can be analytically solved [67], one has $\overleftrightarrow{\sigma}_a \cdot \mathbf{n}|_{r=R} = -\frac{3\mu}{2R}\mathbf{V}_a$ and $\mathbf{F}_a = -6\pi\mu R \mathbf{V}_a$. Inserting these expressions into Eq. (13), one arrives at [28,30]

$$\mathbf{V} = -\frac{1}{4\pi R^2} \int\limits_{|\mathbf{r}|=R} dS\, \mathbf{u}_s := -\langle \mathbf{u}_s \rangle \,, \tag{14}$$

i.e., the velocity of the particle is the negative of the phoretic slip averaged over the surface of the sphere. This result can then be particularized for a specific model of chemically active particles, i.e., specified activity ($K(\mathbf{r}_P)$) and phoretic mobility ($b(\mathbf{r}_P)$) functions. For example, one can choose $K(\mathbf{r}_P)$ to be equal to a constant $\mathcal{K}$ at the catalytic part and zero at the inert part (the so-called "constant flux" condition), and the phoretic mobility to be a constant b over the whole surface. We leave it to the reader to verify that after solving the diffusion equation (Eq. (9)) and calculating the phoretic slip (Eq. (8a)), the surface average in Eq. (14) leads to [30,34]

$$\mathbf{V} = \frac{b\mathcal{K}}{D} \frac{1 - \cos^2 \theta_0}{4} \mathbf{e}_z \,. \tag{15}$$

3 Self-diffusiophoresis near hard walls

In experimental studies, chemically active Janus colloids operate within vessels and therefore during their motion they may reach the vicinity of the walls bounding the solution. We continue with the simple model of a diffusiophoretic, spherical, and active Janus colloid as discussed at the end of the previous section and consider the situation that it operates near a planar wall. (A detailed discussion of the case of mechanically propelled swimmers – i.e., not moving by gradients of thermodynamic fields – near surfaces is provided by the minireview [70] in this topical issue.) The active particle "senses" and responds to the presence of the boundary via the chemical and hydrodynamic fields it creates. First, the wall is impenetrable to the solute released by the particle, and this induces changes in the distribution of the solute number density at the particle surface. The change in the solute distribution leads to changes in the phoretic slip at the particle surface, which translate into changes in the hydrodynamic flow induced by the particle. Second, hydrodynamically the particle creates disturbance flows in the fluid, and these flows are reflected by the no-slip boundary at the walls, coupling back to the particle. The feedback loop between sensing and response is expected to depend on the surface chemistry (e.g., how much of the surface of the particle is covered by catalyst), and can give rise to a rich behavior comprising, in particular, certain surface bound, stable steady-states of motion [45]. The emergence of such steady-states is a complex phenomenon because it requires that the phoretic slip at the particle varies around its surface in such a way that it cancels the hydrodynamic rotation (spinning) which usually accompanies a translation of the particle parallel to the wall, e.g., due to being driven by an external force.

This diffusiophoresis problem can be straightforwardly approached by using the formalism discussed in Sect. 2: adding to Eq. (9) the boundary condition of impenetrability at the wall; adding to Eq. (10) the no-slip boundary condition at the wall; using the Lorentz reciprocal theorem directly in the form of Eq. (13) (which is possible since the corresponding integrals over the surface of the wall vanish due to the no-slip boundary condition in both the active particle and the auxiliary problem) [45]. For a uniform phoretic mobility $b < 0$ (i.e., repulsive interactions between the solute and

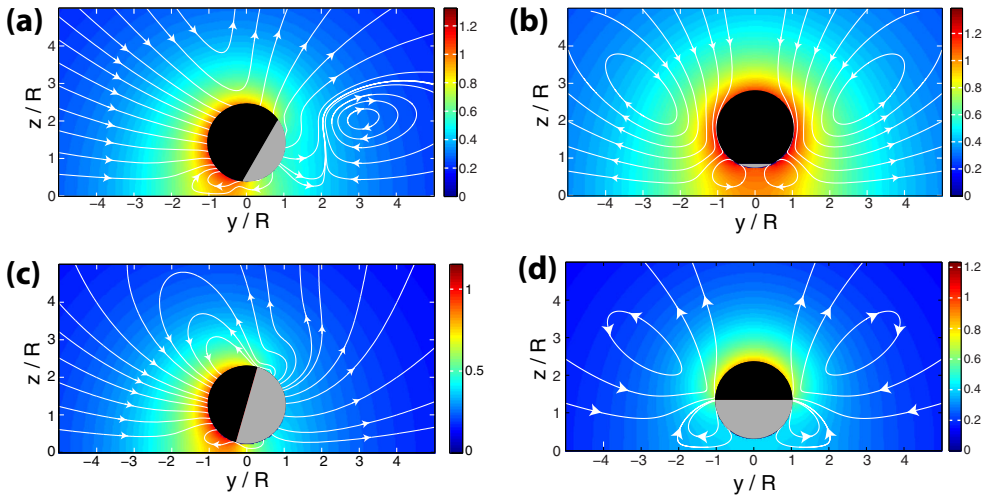

Fig. 2. A chemically active Janus sphere in sliding [(a),(c)] and hovering [(b),(d)] states. The planar wall is located at $z = 0$. The spherical-cap area covered by catalyst is indicated in black (correspondingly, the gray area denotes the chemically-inert part); the coverage by catalyst (i.e., the opening angle θ_0 of the corresponding spherical cap, see Fig. 1(b)) is given by $\theta_0 \simeq 114^\circ$ (panel (a)), $\theta_0 \simeq 154^\circ$ (panel (b)), and $\theta_0 = 90^\circ$ (panels (c), (d)). The corresponding phoretic mobility $b(\mathbf{r})$ is a constant $b < 0$ over the whole surface (panels (a), (b)), or takes different values $b_{cap} < 0$ and b_{inert} over the active cap and the inert regions, respectively (panels (c), (d)), with $b_{inert}/b_{cap} = 0.7$ (c) and -0.7 (d), respectively. The streamlines corresponding to the flow field in the spatially fixed coordinate system ("laboratory frame") are shown as white lines, while the color coding represents the solute number density $c(\mathbf{r})$ in units of the characteristic density $c_0 = \mathcal{K}R/D$. Note the changes in the structure of the streamlines corresponding to the same type of steady state but for different sets of parameters, when comparing (a) and (c), respectively (b) and (d).

the colloid), one can indeed find two types of such surface bound states if sufficiently more than half of the particle surface is covered by catalyst (see Fig. 1(b) for the parametrization of coverage): (a) a "sliding" state, in which the colloid translates along the wall while keeping a constant height above the wall and a constant orientation of its axis of symmetry (illustrated, for $\theta_0 \simeq 114^\circ$, in Fig. 2(a)); and (b) a "hovering" state, in which the particle is motionless and has its axis of symmetry oriented perpendicular to the wall, while the hydrodynamic flow of the solution is maintained (illustrated, for $\theta_0 \simeq 154^\circ$, in Fig. 2(b)). In both cases there is a complex structure of the solute distribution as well as of the streamlines, mediating the emergence of the steady-state orientation and height above the wall (see also Ref. [71]). The study in Ref. [45] has provided evidence for similar states for more complex model systems, e.g., particles with different phoretic mobilities over the catalytic and inert parts. As an example, in Figs. 2(c) and (d) sliding and hovering states, respectively, are illustrated for the case of a half-covered ($\theta_0 = 90^\circ$) Janus particles with $b_{cap} < 0$ and $b_{inert}/b_{cap} = 0.7$ (c) and -0.7 (d), respectively.

Experimental observations of such surface-bounded states for a few types of chemically active particles and various confining geometries have been reported recently [72–74]. (Note that in these studies the analysis is more involved due to the fact that the force and the torque due to gravity are relevant and thus have to be included in the corresponding force and torque balance (Eq. (6)).) These suggest that the phenomenon may be generic for chemically active particles.

4 Self-diffusiophoresis under external fields or flows

The interplay of self-propulsion and external fields or flows can result in rich behaviors not easily foreseen from the consideration of the active and external driving mechanisms in isolation (see, e.g., the minireviews by Stark [75] and by Clement [76] in this topical issue). For instance, active particles can exhibit *taxis*: under certain conditions, they can reliably reorient and migrate in response to cues (such as gravitational fields [15,77], the topography of bounding surfaces [73,74], externally imposed flows [78], or fluid interface-response flows [79]) in their environment. Here we shall consider the possible effects of gravity and external flow. These effects include negative *gravitaxis*, or migration against the direction of gravity, and negative *rheotaxis*, or migration against the flow direction.

4.1 Gravitaxis

Catalytic Janus particles are typically much heavier than water. The weight of a particle will, in part, determine whether it sediments to the bottom of a device or spends significant time in the bulk. The weight of the particle competes against Brownian noise, which promotes diffusion into the bulk, and "swimming activity", which, when the active velocity of the particle is oriented against gravity, promotes escape from a bottom surface. The relative significance of gravity and thermal noise can be quantified by the Péclet number $Pe_g = v_g R/D_P$, where v_g is the settling velocity of a passive particle of radius R and D_P is its diffusion coefficient. The settling velocity can be estimated by balancing the Stokes drag $F_D = 6\pi\mu R v_g$ with the gravitational (buoyancy) force F_g. Using the "eggshell" model of a Janus particle [77], in which the thickness of the catalytic cap is greatest at the particle pole and smoothly decreases to zero at the "equator", one obtains the expression $F_g = \frac{2}{3}\pi t R^2(\rho_{cap} - \rho_{water})g + \frac{4}{3}\pi R^3(\rho_{inert} - \rho_{water})g$, where t is the maximum thickness of the cap. For a polystyrene particle ($\rho_{inert} = 1050\,\mathrm{kg/m^3}$) with $R = 2.5\,\mu$m and a platinum cap ($\rho_{cap} = 21450\,\mathrm{kg/m^3}$) of $t = 5\,$nm in water, one obtains $v_g = 0.66\,\mu$m/s and $Pe_g \approx 28$. If the particle has a silica core ($\rho_{inert} = 2650\,\mathrm{kg/m^3}$) instead of polystyrene, one obtains $v_g = 22.7\,\mu$m/s and $Pe_g \approx 500$. For both particles, the effect of thermal noise is significantly smaller than the effect of gravity. On the other hand, the relative significance of gravity and self-propulsion can be estimated by comparing the corresponding v_g with the contribution of self-propulsion to the particle velocity. A typical phoretic velocity in bulk liquid is $V \sim 5\,\mu$m/s. Here we find a significant difference: the silica particle will sediment but a polystyrene particle can escape gravity.

This type of Janus particle is not only heavy, but also bottom (Pt side) heavy, owing to its inhomogeneous composition. Assuming $b < 0$ (the particle tends to move away from the cap), the bottom-heaviness will tend to align the particle to move upward, i.e., against gravity. The contribution of bottom-heaviness to the angular velocity Ω_g of the particle can be estimated by balancing a Stokes drag torque $\tau_D = 8\pi\mu R^3\Omega_g$ with a gravitational torque $\tau_g = \frac{2}{3}\pi R^2 t\rho_{cap} g y_{cm}\sin(\psi)$, where $y_{cm} \approx 3/4(R + t)$ [77], and ψ is the orientation of the propulsion axis with respect to the vertical. (We note that the density of water does not appear in this expression because the fluid pressure does not exert a torque on the particle.) For both particles, the maximum value of Ω_g, occurring at $\psi = 90°$, is $\Omega_g \approx 3.7\,$deg/s.

These effects have indeed been observed experimentally [77]: orientation and motion of active Janus particles were found to be biased upward, against gravity, and larger particles exhibited a greater bias than smaller ones. A more complex experimental realization, combined with a theoretical analysis, was reported by ten Hagen

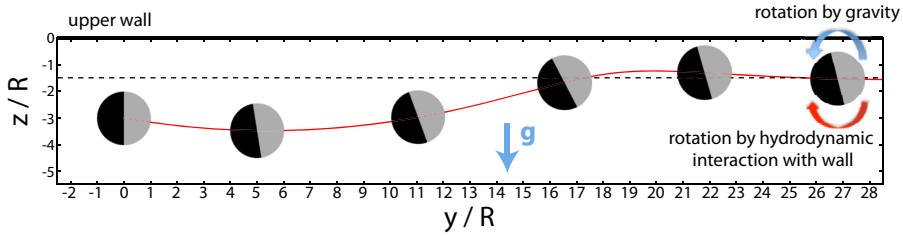

Fig. 3. Numerical studies show that bottom-heaviness can induce "sliding" states for self-diffusiophoretic particles. The bottom heavy Janus particle (polystyrene core, as described in the main text) escapes gravity and reaches the upper surface. The mechanism leading to the steady state is depicted at the right side of the figure.

et al., who used L-shaped active particles, instead of bottom-heaviness, to explore shape asymmetry as an alternative route to gravitaxis [15].

If the particle can escape gravity, some additional interesting effects are possible. Experimentally, it has been observed that active catalytic particles accumulate at upper surfaces [62]. As shown in Fig. 3, the simple model of diffusiophoretic propulsion of a bottom heavy Janus particle discussed above can capture such an effect: a particle is attracted to a steady orientation and constant distance from an upper wall (i.e., a "sliding state.") The mechanism sustaining the steady orientation is depicted in Fig. 3. The bottom-heaviness of the particle contributes a counter-clockwise component to the angular velocity of the particle, tending to rotate the cap away from the wall. On the other hand, the hydrodynamic interaction with the wall always tends to rotate the cap towards the wall. These two contributions[8] exactly cancel if the particle is in the sliding orientation. Simultaneously, the particle achieves a steady height through hydrodynamic interaction with the wall.

4.2 Rheotaxis

This subsection deals with the effect of external flow on the behavior of active colloids and the possibility of rheotaxis. Several decades of study have established that spermatozoa can achieve negative rheotaxis in the presence of flow and bounding surfaces (see, e.g., Refs. [80,81]). The mechanism is elegant and intuitive. Sperm heads tend to be attracted to surfaces. If a sperm head is attracted to a surface, it can act as a "pivot" for the whole spermatozoan. The tail, pointing into the bulk, is in a region of stronger flow than the head. Consequently, the whole spermatozoan is rotated around the head, like a weather vane, so that the tail points downstream. In this orientation, the spermatozoan swims upstream.

However, the "weather vane" mechanism can only apply to elongated particles. Thus the issue arises whether a *spherical* catalytic Janus particle can also exhibit rheotaxis. Based on the results of Sect. 3, one can anticipate a possible route to rheotaxis for a "hoverer." The envisaged mechanism is shown in Fig. 4(a). There we consider a particle which in a quiescent fluid is in a hovering state. The application of an external shear flow tends to rotate the particle clockwise. However, the

[8] For this model of a chemically active particle with *uniform* phoretic mobility b the wall reflected density field contributes only to changes in the distribution of phoretic slip. When $b(\mathbf{r})$ is not constant over the surface, an additional contribution – of the same order of magnitude as the other two – to the rotation of the symmetry axis occurs due to the coupling of the gradient of the wall-reflected density field with the non-uniform phoretic mobility (see Refs. [45,58,74]).

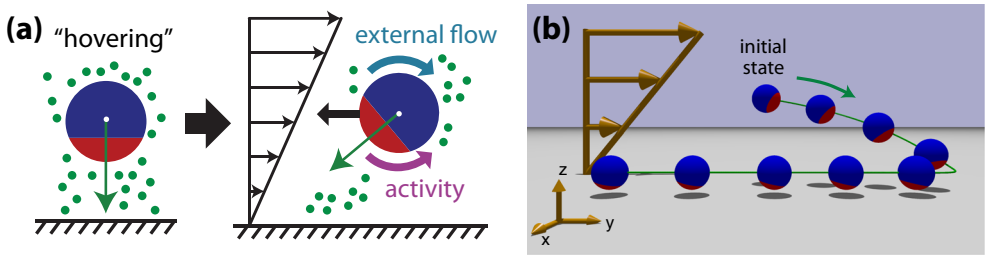

Fig. 4. (a) A schematic illustration of a mechanism to achieve a rheotactic state. A "hovering" particle (left panel) tends to rotate (right panel, blue arrow) when exposed to an external shear flow (right panel, thin black arrows). The chemical activity response of the particle near the wall induces an opposite rotation (right panel, magenta arrow) back towards the (stable in the absence of the flow) hovering state. The two contributions to particle rotation may balance at a certain orientation (right panel, depicted by equal lengths of the blue and magenta arrows), and a steady orientation angle emerges; simultaneously, the particle achieves a steady height above the wall. As a result, the particle translates upstream (medium size black arrow), with its catalytic cap (blue) oriented slightly downstream. (b) Example of a numerically calculated trajectory for a hoverer near a wall reaching a rheotactic state in external flow.

near-surface self-diffusiophoretic activity of the particle tends to rotate the particle back to the hovering state. For small deviations from the hovering orientation, this active contribution is expected to strengthen as the deviation from the hovering orientation increases. Therefore, there should be a steady orientation in which the two contributions balance. Additionally, this orientation is expected to be stable: for larger (smaller) deviations from the hovering orientation, the contribution from the activity is stronger (weaker) than from shear. Simultaneously, the particle attains a steady and stable height above the wall due to the solute "cushion" effect illustrated in Fig. 2. Finally, because the cap is oriented slightly downstream, the particle moves upstream if self-propulsion is strong enough to overcome the external flow.

This intuitive picture leads to the expectation that there is a rheotactic steady state, which is stable against perturbations within the shear plane, i.e., vertical translations of the particle or rotations of the particle orientation vector within the shear plane. However, because the particle is spherical, it is not obvious whether the rheotactic state is stable against perturbations of the orientation vector *out* of the shear plane. In order to proceed from this intuitive picture to a quantitative investigation, the equations of motion for the particle position and orientation can be constructed by linear superposition. As discussed in Ref. [78], the full problem can be divided into two subproblems. In the first subproblem, an active spherical particle moves via self-diffusiophoresis through a quiescent fluid near a planar surface. This subproblem has been already solved in Sect. 3. In the second subproblem, a passive sphere is driven by an external shear flow near a planar surface. This subproblem has been solved by Brenner et al. [82]. The equations describing the motion of the self-diffusiophoretic particle exposed to the external flow are then obtained by summing the corresponding contributions to the translational and rotational velocities from each subproblem (i.e., following from linear superposition). With the full equations at hand, one can examine, via linearization, the stability of the rheotactic state against out-of-plane rotations of the orientation vector. Within this approach, it was shown that, in fact, the near-surface self-diffusiophoresis of a spherical particle can stabilize a rheotactic state if, in that state, the particle is oriented upstream and towards the surface. This criterion matches the situation depicted in Fig. 4(a, right), and the numerical

integration of the equations of motion confirms that a hoverer can indeed exhibit rheotaxis, as illustrated by the trajectory shown in Fig 4(b).

5 Concluding remarks

These succinct notes on the self-diffusiophoretic motion of chemically active particles are supposed to capture a significant part of the complexity and richness of this topic. Due to the limited space, various interesting aspects and results have not been addressed. Here we list some of these issues, also covered by the references provided. (i) The effects of thermal fluctuations, leading to rotational diffusion of the colloid, have not been analyzed. As discussed, e.g., in Refs. [7,36,83] for particles with axial symmetry (in which case self-diffusiophoresis leads only to translation), due to rotational diffusion of the axis of symmetry the motion crosses over from a ballistic regime at timescales shorter than the rotational diffusion time of the particle to diffusion with an "activity enhanced" effective diffusion coefficient at long times. (ii) The simple model analyzed in Sect. 2 for a Janus sphere predicts a velocity which is independent of the size of the colloid. References [38,40] show that this result is the zeroth order term of the solution for surface films of non-vanishing thickness. This means that corrections in δ/R become important as the radius of the colloid decreases [84]. Reference [37] has shown that accounting for chemical kinetics which are not completely reaction-limited, i.e., $Da \neq 0$, also leads to a dependence of the phoretic velocity on the particle size; this theoretically predicted dependence agrees well with the experimental observations. (iii) The dimer model (i.e., a fully catalytic sphere rigidly connected to an inert one) introduced in Ref. [32] (see also, e.g., Refs. [33,35,44]), is sufficiently simple to allow for analytic solutions. It reveals the strong effects which the shape of the particle can have on the emerging solute density gradients. It highlights the complex nature of the hydrodynamic flows associated with self-diffusiophoresis.

We conclude by mentioning two interesting areas which so far have been less explored. First, little is known about the behavior of chemically active particles near or at soft interfaces. The interplay between the chemical activity and the response of a soft interface may lead to a very rich phenomenology [46,48,55,79]. Second, we expect that self-diffusiophoresis of chemically active colloids in complex fluids (e.g., liquid crystals, or visco-elastic liquids) could become another topic of increasing interest, motivated by applications towards biology or chemical engineering.

References

1. R.F. Ismagilov, A. Schwartz, N. Bowden, G.M. Whitesides, Angew. Chem. Int. Ed. **41**, 652 (2002)
2. W.F. Paxton, K.C. Kistler, C.C. Olmeda, A. Sen, S.K. St.Angelo, Y.Y. Cao, T.E. Mallouk, P.E. Lammert, V.H. Crespi, J. Am. Chem. Soc. **126**, 13424 (2004)
3. G.A. Ozin, I. Manners, S. Fournier-Bidoz, A. Arsenault, Adv. Mater. **17**, 3011 (2005)
4. W.F. Paxton, S. Sundararajan, T.E. Mallouk, A. Sen, Angew. Chem. Int. Ed. **45**, 5420 (2006)
5. A.A. Solovev, Y.F. Mei, E.B. Urena, G.S. Huang, O.G. Schmidt, Small **5**, 1688 (2009)
6. T. Mirkovic, N.S. Zacharia, G.D. Scholes, G.A. Ozin, Small **6**, 159 (2010)
7. J.R. Howse, R.A.L. Jones, A.J. Ryan, T. Gough, R. Vafabakhsh, R. Golestanian, Phys. Rev. Lett. **99**, 048102 (2007)
8. L. Tung-Chun, M. Alarcón-Correa, C. Miksch, K. Hahn, J.G. Gibbs, P. Fischer, Nano Lett. **14**, 2407 (2014)
9. J. Palacci, S. Sacanna, A.S. Steinberg, D.J. Pine, P.M. Chaikin, Science **339**, 936 (2013)

10. L. Baraban, M. Tasinkevych, M.N. Popescu, S. Sánchez, S. Dietrich, O.G. Schmidt, Soft Matter **8**, 48 (2012)
11. W. Gao, A. Uygun, J. Wang, J. Am. Chem. Soc. **134**, 897 (2012)
12. H.-R. Jiang, N. Yoshinaga, M. Sano, Phys. Rev. Lett. **105**, 268302 (2010)
13. B. Qian, D. Montiel, A. Bregulla, F. Cichos, H. Yang, Chem. Sci. **4**, 1420 (2013)
14. I. Buttinoni, G. Volpe, F. Kümmel, G. Volpe, C. Bechinger, J. Phys.: Cond. Matter **24**, 284129 (2012)
15. B. ten Hagen, F. Kümmel, R. Wittkowski, D. Takagi, H. Löwen, C. Bechinger, Nat. Comm. **5**, 4829 (2014)
16. S.J. Ebbens, J.R. Howse, Soft Matter **6**, 726 (2010)
17. Y. Hong, D. Velegol, N. Chaturvedi, A. Sen, Phys. Chem. Chem. Phys. **12**, 1423 (2010)
18. S. Sánchez, L. Soler, J. Katuri, Angew. Chem. Int. Ed. **54**, 1414 (2015)
19. E.M. Purcell, Am. J. Phys. **45**, 3 (1977)
20. E. Lauga, T.R. Powers, Rep. Prog. Phys. **72**, 096601 (2009)
21. S. Spagnolie, E. Lauga, Phys. Fluids **22**, 081902 (2010)
22. S.E. Spagnolie, E. Lauga, J. Fluid Mech. **700**, 105 (2012)
23. C.M. Pooley, G.P. Alexander, J.M. Yeomans, Phys. Rev. Lett. **99**, 228103 (2007)
24. R. Golestanian, J.M. Yeomans, N. Uchida, Soft Matter **7**, 3074 (2011)
25. A. Zöttl, H. Stark, Phys. Rev. Lett. **108**, 218104 (2012)
26. R.G. Winkler, Eur. Phys. J. Special Topics **225**, 2079 (2016)
27. M.E. Cates, J. Tailleur, Ann. Rev. Cond. Matter Phys. **6**, 219 (2015)
28. R. Golestanian, T.B. Liverpool, A. Ajdari, Phys. Rev. Lett. **94**, 220801 (2005)
29. A. Ajdari L. Bocquet, Phys. Rev. Lett. **96**, 186102 (2006)
30. R. Golestanian, T.B. Liverpool, A. Ajdari, New J. Phys. **9**, 126 (2007)
31. F. Jülicher, J. Prost, Eur. Phys. J. E **29**, 27 (2009)
32. G. Ruckner, R. Kapral, Phys. Rev. Lett. **98**, 150603 (2007)
33. Y.G. Tao, R. Kapral, J. Chem. Phys. **128**, 164518 (2008)
34. M.N. Popescu, S. Dietrich, M. Tasinkevych, J. Ralston, Eur. Phys. J. E **31**, 351 (2010)
35. M.N. Popescu, M. Tasinkevych, S. Dietrich, EPL **95**, 28004 (2011)
36. R. Golestanian, Phys. Rev. Lett. **102**, 188305 (2009)
37. S. Ebbens, M.-H. Tu, J. Howse, R. Golestanian, Phys. Rev. E **85**, 020401(R) (2012)
38. B. Sabass, U. Seifert, J. Chem. Phys. **136**, 064508 (2012)
39. B. Sabass, U. Seifert, J. Chem. Phys. **136**, 214507 (2012)
40. N. Sharifi-Mood, J. Koplik, C. Maldarelli, Phys. Fluids **25**, 012001 (2013)
41. D.G. Crowdy, J. Fluid Mech. **735**, 473 (2013)
42. R. Soto, R. Golestanian, Phys. Rev. E **91**, 052304 (2015)
43. S. Michelin, E. Lauga, Eur. Phys. J. E **38**, 7 (2015)
44. S.Y. Reigh, R. Kapral, Soft Matter **11**, 3149 (2015)
45. W. Uspal, M. Popescu, S. Dietrich, M. Tasinkevych, Soft Matter **11**, 434 (2015)
46. H. Masoud, H. Stone, J. Fluid Mech. **741**, R4 (2014)
47. T. Bickel, A. Majee, A. Würger, Phys. Rev. E **88**, 012301 (2013)
48. A. Würger, J. Fluid Mech. **752**, 589 (2014)
49. J. de Graaf, G. Rempfer, C. Holm, IEEE Trans. NanoBiosci. **14**, 272 (2015)
50. J.F. Joanny, F. Jülicher, K. Kruse, J. Prost, New J. Phys. **9**, 422 (2007)
51. J. Palacci, C. Cottin-Bizonne, C. Ybert, L. Bocquet, Phys. Rev. Lett. **105**, 088304 (2010)
52. I. Theurkoff, C. Cottin-Bizonne, J. Palacci, C. Ybert, L. Bocquet, Phys. Rev. Lett. **108**, 268303 (2012)
53. H.H. Wensink, J. Dunkel, S. Heidenreich, K. Drescher, R.E. Goldstein, H. Löwen, J.M. Yeomans, Proc. Natl. Acad. Sci. **109**, 14308 (2012)
54. M.C. Marchetti, J.F. Joanny, S. Ramaswamy, T.B. Liverpool, J. Prost, M. Rao, R.A. Simha, Rev. Mod. Phys. **85**, 1143 (2013)
55. H. Masoud, M. Shelley, Phys. Rev. Lett. **112**, 128304 (2014)
56. F. Ginot, I. Theurkauff, D. Levis, C. Ybert, L. Bocquet, L. Berthier, C. Cottin-Bizonne, Phys. Rev. X **5**, 011004 (2015)
57. J. Elgeti, R.G. Winkler, G. Gompper, Rep. Prog. Phys. **78**, 056601 (2015)

58. J. Anderson, Ann. Rev. Fluid Mech. **21**, 61 (1989)
59. K. Kroy, D. Chakraborty, F. Cichos, Eur. Phys. J. Special Topics **225**, 2207 (2016)
60. R. Seemann, J.-B. Fleury, C.C. Maass, Eur. Phys. J. Special Topics **225**, 2227 (2016)
61. B. Derjaguin, Y. Yalamov, A. Storozhilova, J. Colloid Interface Sci. **22**, 117 (1966)
62. A. Brown, W. Poon, Soft Matter **10**, 4016 (2014)
63. S. Ebbens, D. Gregory, G. Dunderdale, J. Howse, Y. Ibrahim, T. Liverpool, R. Golestanian, EPL **106**, 58003 (2014)
64. S.R. de Groot, P. Mazur, *Non-equilibrium Thermodynamics* (North-Holland, Amsterdam, 1962)
65. S. Michelin, E. Lauga, J. Fluid Mech. **747**, 572 (2014)
66. S. Kim, S.J. Karrila, *Microhydrodynamics: Principles and Selected Applications* (Butterworth-Heinemann, Boston, 1991)
67. J. Happel, H. Brenner, *Low Reynolds number hydrodynamics* (Noordhoff Int. Pub., 1973)
68. H.A. Stone, A. Samuel, Phys. Rev. Lett. **77**, 4102 (1996)
69. C. Pozrikidis, *A Practical Guide to Boundary Element Methods with the Software Library BEMLIB* (CRC Press, Boca Raton, 2002)
70. J. Elgeti, G. Gompper, Eur. Phys. J. Special Topics **225**, 3033 (2016)
71. A. Mozaffari, N. Sharifi-Mood, J. Koplik, C. Maldarelli, Phys. Fluids **28**, 053107 (2016)
72. A. Brown, I. Vladescu, A. Dawson, T. Vissers, J. Schwarz-Linek, J. Lintuvuori, W. Poon, Soft Matter **12**, 131 (2016)
73. S. Das, A. Garg, A. Campbell, J. Howse, A. Sen, D. Velegol, R. Golestanian, S. Ebbens, Nat. Comm. **6**, 8999 (2015)
74. J. Simmchen, J. Katuri, W. Uspal, M. Popescu, M. Tasinkevych, S. Sánchez, Nat. Comm. **7**, 10598 (2016)
75. H. Stark, Eur. Phys. J. Special Topics **225**, 3069 (2016)
76. E. Clement, A. Lindner, C. Douarche, H. Auradou, Eur. Phys. J. Special Topics **225**, 3089 (2016)
77. A. Campbell, S. Ebbens, Langmuir **29**, 14066 (2013)
78. W.E. Uspal, M.N. Popescu, S. Dietrich, M. Tasinkevych, Soft Matter **11**, 6613 (2015)
79. A. Domínguez, P. Malgaretti, M.N. Popescu, S. Dietrich, Phys. Rev. Lett. **116**, 078301 (2016)
80. F.P. Bretherton, L. Rothschild, Proc. R. Soc. London B **153**, 490 (1961)
81. K. Miki, D.E. Clapham, Curr. Biol. **23**, 443 (2013)
82. A. Goldman, R. Cox, H. Brenner, Chem. Eng. Sci. **22**, 653 (1967)
83. B. ten Hagen, S. van Teeffelen, H. Löwen, J. Phys.: Condens. Matter **23**, 194119 (2011)
84. P. Colberg, S. Reigh, B. Robertson, R. Kapral, Acc. Chem. Res. **47**, 3504 (2014)